



Hot Deformation Behavior of a Novel Near- β Titanium Alloy Ti-5.5Mo-6V-7Cr-4Al-2Sn-1Fe in ($\alpha + \beta$) Phase Region

Jinyang Gai^{1,2}, Jun Cheng^{2,3*}, Jinshan Li³, Zhaoxin Du⁴, Wen Zhang², Sen Yu² and Zhentao Yu^{5*}

¹ School of Material Science and Engineering, Northeastern University, Shenyang, China, ² Shaanxi Key Laboratory of Biomedical Metal Materials, Northwest Institute for Non-ferrous Metal Research, Xi'an, China, ³ State Key Laboratory of Solidification Processing, Northwestern Polytechnical University, Xi'an, China, ⁴ School of Materials Science and Engineering, Inner Mongolia University of Technology, Hohhot, China, ⁵ Institute of Advanced Wear and Corrosion Resistant and Functional Materials, Jinan University, Guangzhou, China

OPEN ACCESS

Edited by:

Weijie Lu,
Shanghai Jiao Tong University, China

Reviewed by:

Fengcang Ma,
University of Shanghai for Science and
Technology, China
Changjiang Zhang,
Taiyuan University of
Technology, China
Liang-Yu Chen,
Jiangsu University of Science and
Technology, China

*Correspondence:

Jun Cheng
524161386@qq.com
Zhentao Yu
ninyzt@163.com

Specialty section:

This article was submitted to
Structural Materials,
a section of the journal
Frontiers in Materials

Received: 04 November 2019

Accepted: 17 December 2019

Published: 14 January 2020

Citation:

Gai J, Cheng J, Li J, Du Z, Zhang W,
Yu S and Yu Z (2020) Hot Deformation
Behavior of a Novel Near- β Titanium
Alloy Ti-5.5Mo-6V-7Cr-4Al-2Sn-1Fe in
($\alpha + \beta$) Phase Region.
Front. Mater. 6:343.
doi: 10.3389/fmats.2019.00343

The hot deformation behavior of a novel near-beta titanium alloy Ti-5.5Mo-6V-7Cr-4Al-2Sn-1Fe in ($\alpha + \beta$) phase region in the temperature of 605~755°C and strain rate range of $10^{-3} \sim 10^{-1} / s^{-1}$ was investigated on the Gleeble-3800 thermo-mechanical simulator. The results showed that the deformation parameters can have a significant influence on flow softening behavior and the microstructure evolution, as well as dynamic recrystallization is remarkable at temperature 755°C and strain rate $10^{-3} s^{-1}$. The flow stress decreases with the increase of temperature and decrease of strain rate. With the rise of temperature and strain rate, the content of α phase gradually decreases. During the thermal deformation process, the α phase content decreases with the increase of the strain rate and the size of α phase decreases with increasing temperature. α_{GB} is short rod or spherical. And α phase precipitated after short-term aging preferentially nucleated within the grains after aging treatment. Moreover, the thermal-mechanical process does not induce α phase generation compared to general heat treatment.

Keywords: near-beta titanium alloy, hot deformation behavior, flow softening, α phase spheroidized, microstructure evolution

INTRODUCTION

Near- β titanium alloys have been widely used in aviation, medical, petrochemical and other fields owing to its low density, high specific strength, excellent match of strength, ductility and toughness (Qin et al., 2018; Zhang and Chen, 2019). The microstructure evolution of near- β titanium alloys are extremely sensitive to processing parameters (Zhang et al., 2019), resulting in a narrow processing range. The flow softening refers to the common phenomenon that flow stress decreases remarkably with strain increasing in the hot processing. And the flow softening behaviors have a certain guiding role in the optimization of the forging process for near-beta titanium alloy. Studies have shown that dynamic recovery (DRV) (Luo et al., 2015), dynamic recrystallization (DRX) (Matsumoto et al., 2014), and α phase spheroidization (Jones and Jackson, 2013) are the main causes of flow softening.

Bai et al. (2014) revealed that the main hot deformation mechanism of TLM titanium alloy at 750~850°C was DRV and DRX by building hot processing map. It has been studied that the Ti-55531 alloy was deformed in the ($\alpha + \beta$) region by Warchomicka et al. (2011). Due to the existence of the α phase, the dislocation motion and the formation of the β -subcrystal are hindered, and the transition from the low-angle grain boundaries (LAGBs) to the high-angle grain boundaries (HAGBs) exhibits the characteristics of dynamic recrystallization. In recent years, more studies focus on the phase transition behavior of titanium alloy during hot deformation. Hua et al. (2014) studied the stress-induced phase transition behavior. Their results indicated that the deformation bands and dislocations generation during the thermal deformation process increased the nucleation sites of α phase and promoted the $\beta \rightarrow \alpha$ transition. Fan et al. (2017) explained the spheroidization mechanism of α phase of Ti-7333 alloy during thermal deformation. However, Jonas et al. (2017) found that flow stress reached a peak after thermal deformation and then decreased gradually, and the content of β phase increased. It was considered that the dynamic softening was caused by $\alpha \rightarrow \beta$ transformation. Therefore, it is still necessary to study the microstructure evolution and phase transition behavior in the thermal deformation of near- β titanium alloy.

The present study is carried out to clarify the flow behavior and microstructure evolution of Ti-5.5Mo-6V-7Cr-4Al-2Sn-1Fe in ($\alpha + \beta$) phase region, which provides supportive information on effect of stress on phase transition by comparing aging and thermal deformation.

MATERIALS AND EXPERIMENTAL PROCEDURES

The alloy used in this experiment was produced by three times of vacuum self-consumable arc melting (VAR), and its chemical composition was Ti-5.4Mo-5.9V-7.1Cr-3.8Al-1.8Sn-1.1Fe (wt%). The ingot is forged by forging and repeatedly drawn to obtain a bar with a diameter of 50 mm. The β transus temperature was measured to be about 765°C by metallographic observation. Cylindrical specimens of $\Phi 8 \times 12$ mm by wire cut from the bar were solution-treated at 850°C for 30 min by air cooling, and the microstructure of experimental alloy after solution treatment is shown in **Figure 1** with β single phase.

The thermal compression test was conducted on Gleeble-3800 thermo-mechanical simulator in the temperature of 605~755°C and strain rate range of $10^{-3} \sim 10^{-1} \text{ s}^{-1}$. Two pieces of Tantalum slices were placed on the specimen and clamp to reduce friction. The samples were heated to a preset temperature at a rate of 10°C/s for 5 min to ensure complete heating and to avoid excessive grain growth. The final compressive deformation was 80%. The specimens were immediately quenched to obtain the hot deformation microstructure after the hot compression test. The metallographic samples were cut along the axis, mechanically polished and then etched in Kroll's etching solution of 10% HF, 30% HNO₃ and 60% H₂O. The morphology of α phase was observed by scanning electron microscopy

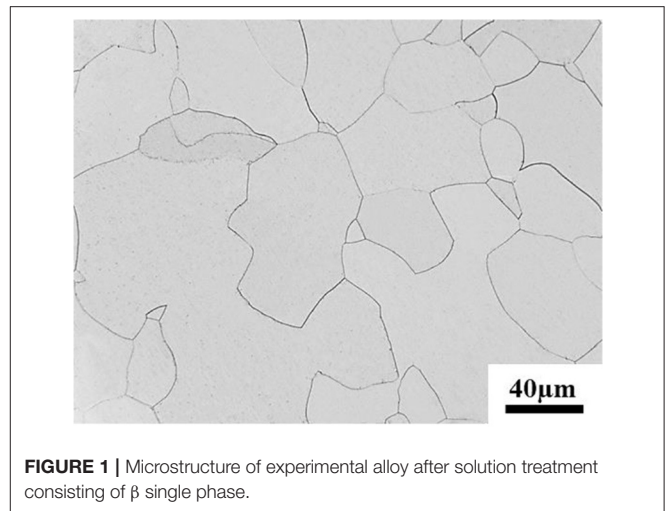


FIGURE 1 | Microstructure of experimental alloy after solution treatment consisting of β single phase.

(SEM) and quantitative analysis was performed using Image-Pro Plus software.

In order to study the effect of stress on the α phase transition, the heat treatment test without stress was also carried out on the Gleeble-3800 thermo-mechanical simulator. The initial processing conditions were the same, and the holding time was consistent with the thermal deformation test at the same temperature. The specific test parameters were shown in **Figure 2**.

RESULTS AND DISCUSSION

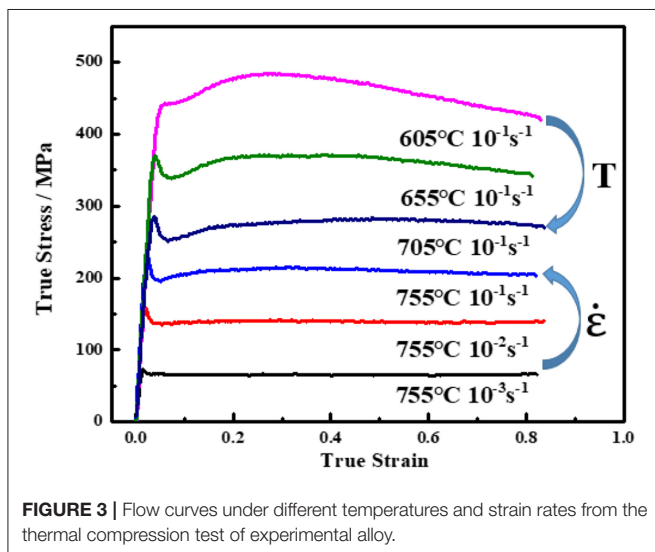
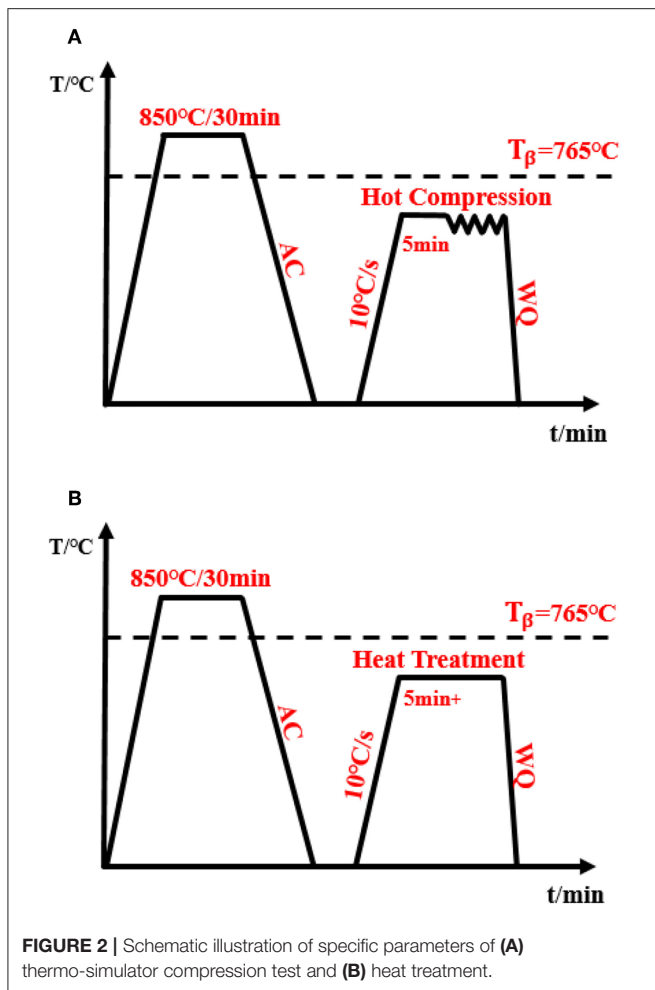
Flow Behavior and Deformation Mechanics

Figure 3 showed the flow stress curves of the experimental alloy Ti-5.5Mo-6V-7Cr-4Al-2Sn-1Fe in the temperature of 605~755°C and strain rate range of $10^{-3} \sim 10^{-1} \text{ s}^{-1}$. At the beginning of deformation, the process is the work hardening stage, where the stress rises almost linearly, and the stress reaches a peak when the strain is very small. It is considered that the rapid proliferation of dislocations is related to the lattice structure and the mechanical parameters of the material, resulting in the insensitivity to parameter variation (Liang et al., 2014). As the degree of deformation increases, the stress gradually decreases, which is called the dynamic softening stage. Since dislocation annihilation and rearrangement strongly depend on the ability of dislocation migration and collision between adjacent dislocations, the process is sensitive to parameters variation. The peak stress gradually decreases with increasing of temperature. When the strain rate increases from 10^{-3} s^{-1} to 10^{-1} s^{-1} , the peak stress gradually increases, appearing the opposite law, as seen in **Figure 4A**. It can be explained according to the dislocation mechanism (Mitchell et al., 2002):

$$\dot{\epsilon} = \rho b v \quad (1)$$

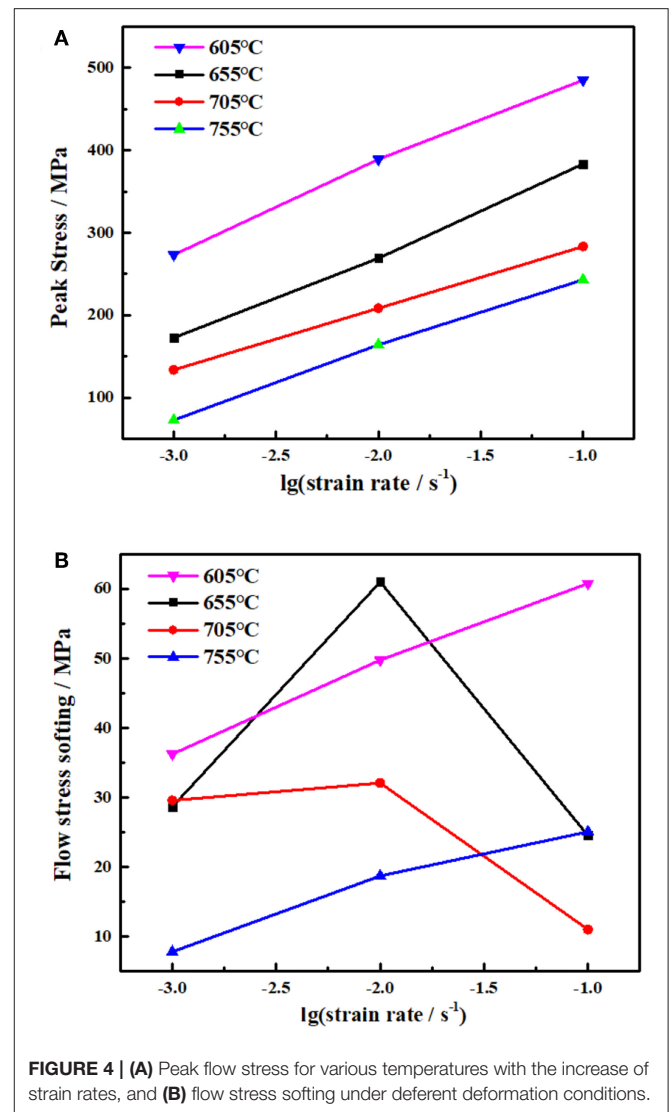
$$v = A \sigma^m \quad (2)$$

where $\dot{\epsilon}$ represents the strain rate, ρ is the density of the movable dislocations, b denotes the Burgers vector, v represents the rate of



proliferation of the movable dislocations, and m is the average of dislocation velocity (Reviewer 2).

As the strain rate increases, the rate of dislocation proliferation increases and the peak stress increases accordingly. After the



relatively slow softening stage, the flow stress gradually stabilizes and reaches a steady state, that is, the dislocation proliferation and annihilation reach a balance. Bai et al. (2014) also found similar results when investigating the thermal deformation of TLM alloy.

Flow softening is often manifested by the decrease of flow stress during compression deformation of high temperature (Sakaki et al., 1994). And the value of flow softening could be expressed as the difference between the peak flow stress and the steady flow stress ($\Delta\sigma = \sigma_p - \sigma_s$. Where: σ_p is the peak stress; σ_s is the steady state stress). **Figure 4B** reflected the variation of flow softening stress with strain rate and temperature. The same law is also basically exhibited at 655 and 755°C. The flow softening value increases first and then decreases with the increase of strain rate, and the flow softening behavior is most obvious at 655°C/ $10^{-2} s^{-1}$. However, when the temperature is 605 and 755°C (close to the phase transition temperature), the amplitude of flow softening increases with increasing strain rate,

which may be due to dynamic recovery (DRV) and dynamic recrystallization (DRX). At present, DRV, DRX and α phase spheroidization have been considered to be the main causes of flow softening phenomenon.

Work hardening and dynamic softening effects are considered interdependent because the dynamic softening driving force is provided by the deformation energy produced by work hardening, and the softening effect causes continuous strain to induce subsequent hardening (Zurob et al., 2014). Although the correlation between work hardening and dynamic softening has been confirmed from the flow curves and microstructure evolution, there is no correlation and quantitative relationship between work hardening and dynamic softening. From the perspective of dislocation, dislocation proliferation and annihilation coexist and compete with each other, so work hardening and flow softening are exhibited in the isothermal compression test. A dynamic model of variation in dislocation density could be used to represent this relationship (Bergström, 1970) as:

$$d\rho/d\varepsilon = U - \Omega\rho \quad (3)$$

where U and Ω are dislocation proliferation and annihilation coefficients, respectively.

According to the dislocation evolution described by Mecking and Kocks (1981) and Estrin and Mecking (1984) models, the variation in dislocation before and after dynamic recrystallization

can be expressed as:

$$d\rho/d\varepsilon = k_1\sqrt{\rho} - k_2\rho \quad (4)$$

$$d\rho/d\varepsilon = k - k_2\rho \quad (5)$$

$$k = k_1\sqrt{\rho_c} = k_1\sigma_c/(\alpha M G b) \quad (6)$$

where α and M represent the Taylor coefficient and the conversion factor, respectively, G is the shear modulus, and σ_c is the critical stress at the beginning of DRX.

Thermal Deformation Microstructure Analysis

Figure 5 exhibited the microstructure of the alloy at different temperatures of 80% deformation and strain rate of 10^{-3} s^{-1} . It could be clearly observed that the grains were elongated perpendicular to the compression direction. And α phase was mainly segregated in the vicinity of the grain boundary, as well as the content of α phase gradually decreases with the increase of temperature. At 755°C, the jagged β grain boundary appeared owing to dynamic recrystallization occurring. And α phase content was close to zero, which could be due to the near phase transition temperature, causing $\alpha \rightarrow \beta$ transformation.

The phenomenon of “ β necking” in Figure 5D was caused by periodic DRV/DRX competition (Ning et al., 2015). Furthermore, it could be found from the SEM photographs Figure 5A that the grain boundaries were still continuous at 605°C. And discontinuous grain boundary α phase (α_{GB}) began

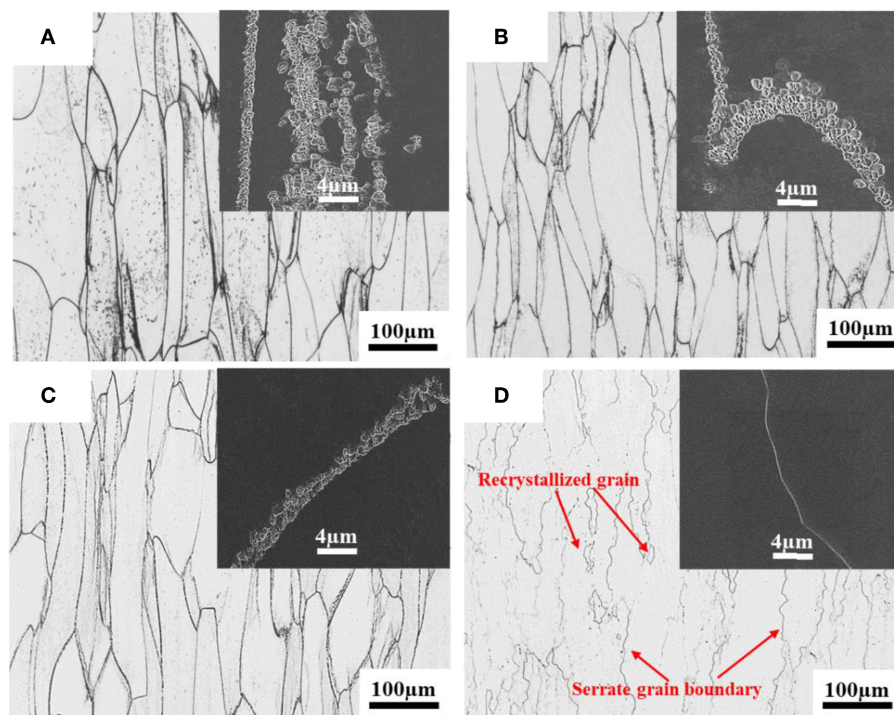


FIGURE 5 | Microstructure after isothermal compression under the strain rate of 10^{-3} s^{-1} with different temperatures of (A) 605°C, (B) 655°C, (C) 705°C, (D) 755°C, and the upper right corners are the SEM images of the grain boundary at the corresponding temperature.

to appear at 655°C, which was short rod or ellipsoid. During the thermal deformation process, the α -phase stable elements aggregated toward the grain boundaries, and the β -phase stable elements were discharged to the inside of the grains while nucleation. In addition, the formation of a large number of crystal defects during the deformation process accelerated the diffusion rearrangement of alloying elements, causing most of α phase to precipitate at the grain boundaries (Reviewer 3).

Microstructures at different strain rates at 655°C were demonstrated in **Figure 6**. When the strain rate increased from 10^{-3} s^{-1} to 10^{-1} s^{-1} , the sub-grain boundaries and sub-grains appeared gradually, and the DRV phenomenon gradually becomes obvious, which caused the dislocation to migrate and multilateralize. Moreover, α phase particles were smaller in size ($\sim 1 \mu\text{m}$) and had a lower precipitation content, which could be due to the shorter strain time, while the higher strain rate, and α phase continued nucleating and growing without sufficient time. An interesting phenomenon could be observed in **Figure 6E**. The spheroidization phenomenon of the α phase was most obvious at the 655°C and 10^{-2} s^{-1} , but when the strain rate was 10^{-1} s^{-1} , α_{GB} had a tendency of “points connected into a line”.

Effect of Stress on α Precipitation Phase

Figure 7 exhibited the microstructure of heat treatment at 655°C, where the aging time was the same as the total time at different strain rates at this temperature, including holding time (5 min) and hot compression time. When the strain

rates were 10^{-1} s^{-1} , 10^{-1} s^{-2} , and 10^{-1} s^{-3} respectively, the total time was 12, 14, and 27 min in turn. The α phase precipitated after short-term aging preferentially nucleated within the grains. The distribution of α phase in the grains was similar to the “sub-grain.” The defect position inside of the grains became the preferential nucleation sites of α phase, not the grain boundaries, which nucleated within the grains. The distribution of α phase in the grains was similar to the “sub-grain.” A more reasonable explanation was related to the deformation zone and the sub-grain formed during high temperature deformation (Chai et al., 2013; Chen et al., 2016). The defect position in the grains became the preferential nucleation site of the α phase, not the grain boundaries, which indicated that the elastic strain energy of the defect location in the alloy contributed more to the nucleation work of the phase than the nucleation work of the grain boundary energy (Chang et al., 2006). It was clearly observed that the positions of the nucleation of α phase were uneven, precipitating easily along the grain boundaries and dislocations. Comparing the hot deformation microstructure (**Figure 6**) and the heat treatment microstructure (**Figure 7**) at 655°C, it could be found that the content of α precipitated phase was significantly different under hot deformation and heat treatment, and the quantitative analysis was shown in the **Figure 8**. Under the same time, the content of α phase was significantly reduced under the condition of isothermal compression, which fully demonstrated that the thermal coupling conditions suppressed the $\beta \rightarrow \alpha$ transition. It was in contrast to the research

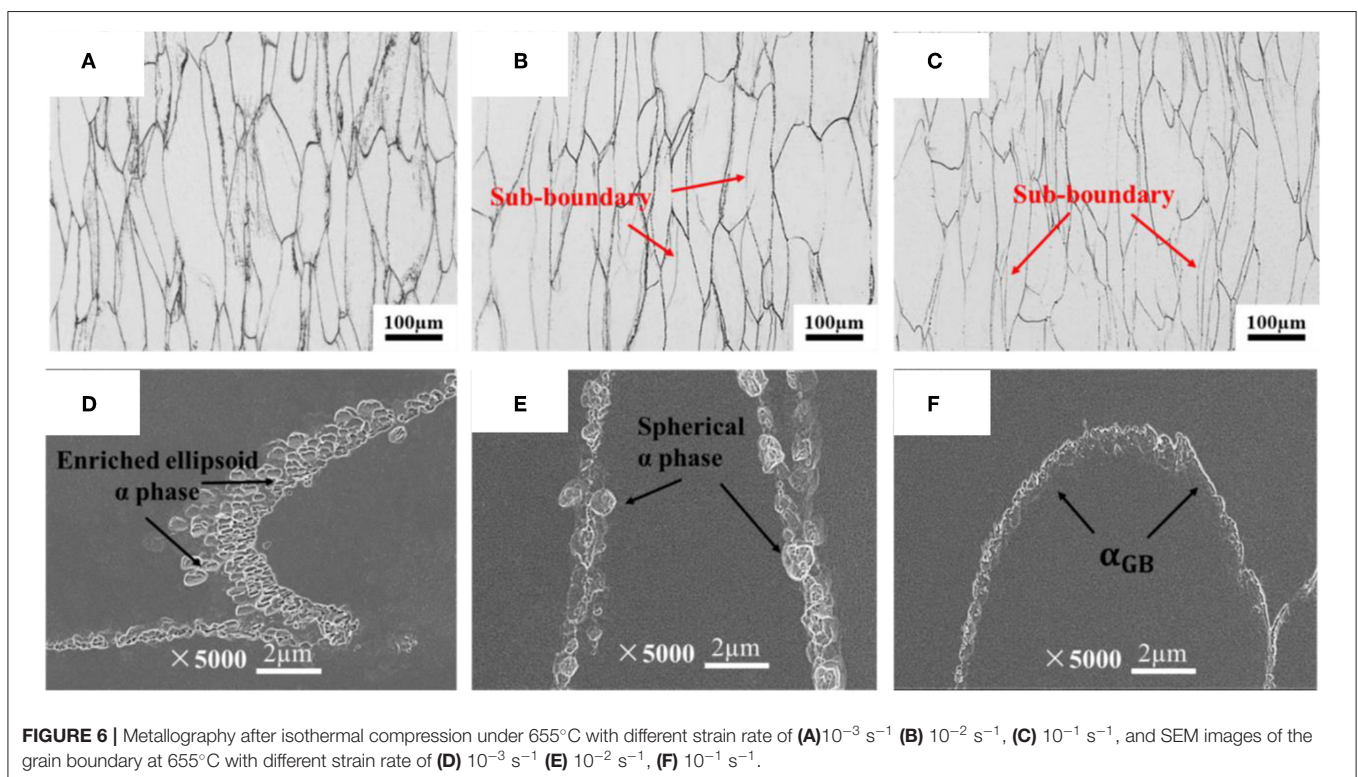


FIGURE 6 | Metallography after isothermal compression under 655°C with different strain rate of (A) 10^{-3} s^{-1} (B) 10^{-2} s^{-1} , (C) 10^{-1} s^{-1} , and SEM images of the grain boundary at 655°C with different strain rate of (D) 10^{-3} s^{-1} (E) 10^{-2} s^{-1} , (F) 10^{-1} s^{-1} .

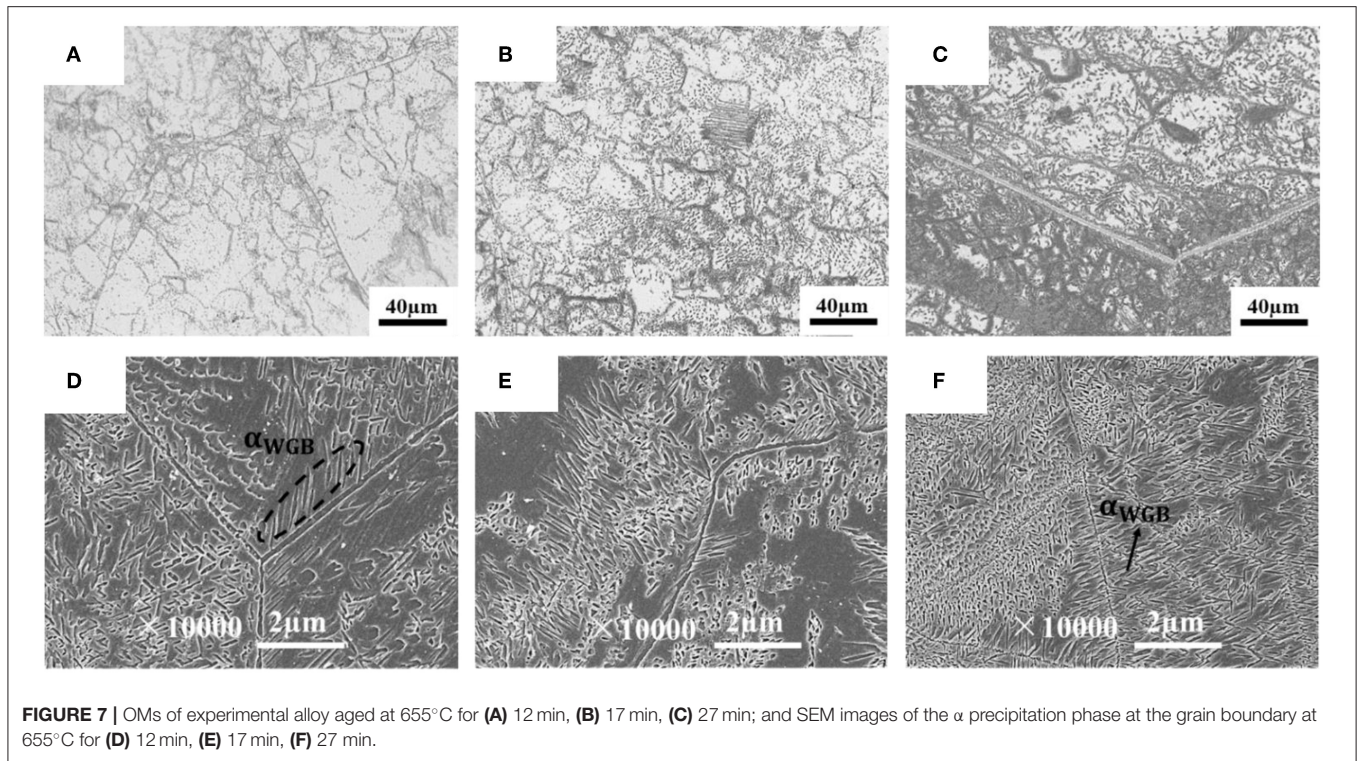


FIGURE 7 | OMs of experimental alloy aged at 655°C for (A) 12 min, (B) 17 min, (C) 27 min; and SEM images of the α precipitation phase at the grain boundary at 655°C for (D) 12 min, (E) 17 min, (F) 27 min.

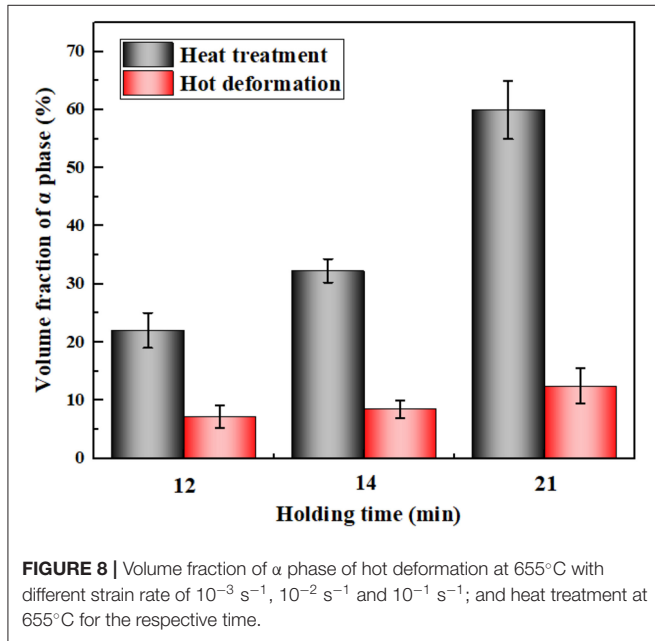


FIGURE 8 | Volume fraction of α phase of hot deformation at 655°C with different strain rate of 10^{-3} s^{-1} , 10^{-2} s^{-1} and 10^{-1} s^{-1} ; and heat treatment at 655°C for the respective time.

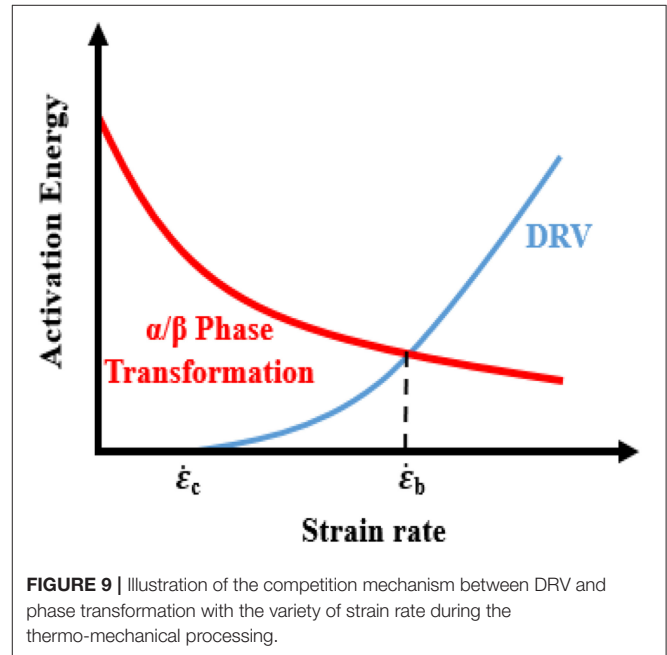


FIGURE 9 | Illustration of the competition mechanism between DRV and phase transformation with the variety of strain rate during the thermo-mechanical processing.

results of Dehghan-Manshadi and Dippenaar (2012), where no so-called dynamic stress-induced phase transition (DSIPT) occurred. Competition between α/β phase transition and DRV and DRX existed in thermal deformation of titanium alloys. It could be seen from the microstructure that the serrated grain boundaries did not occur at 655°C, and the subgrain boundaries

and the subgrains appeared as the strain rate increased, so the DRV process could be considered to suppress DSIPT. There were no rearrangements of alloying elements and variations in crystal structure in DRV process, and dynamic softening could be achieved with a small activation energy. The competitive relationship between this DRV and α/β phase transition for

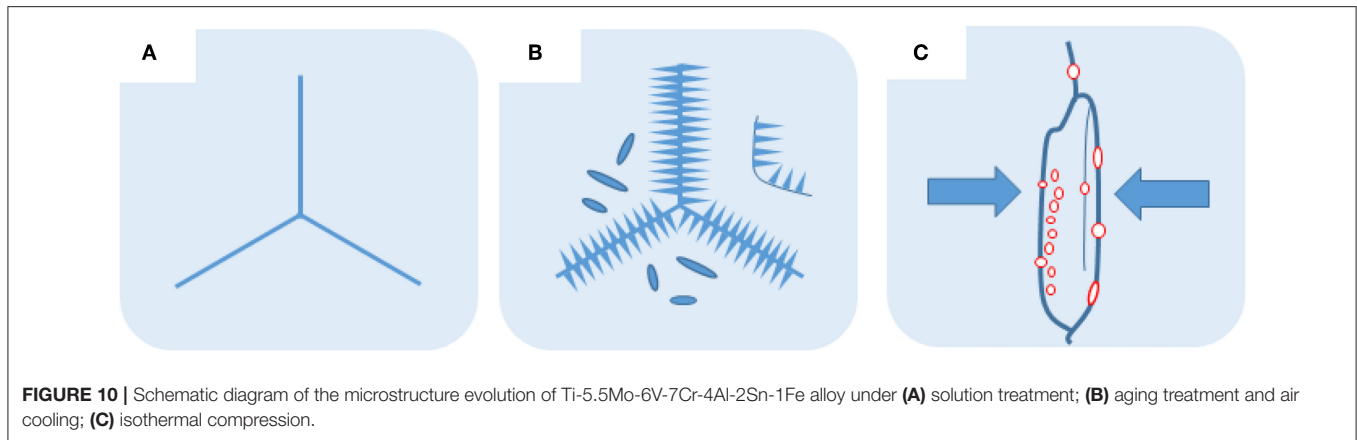


FIGURE 10 | Schematic diagram of the microstructure evolution of Ti-5.5Mo-6V-7Cr-4Al-2Sn-1Fe alloy under (A) solution treatment; (B) aging treatment and air cooling; (C) isothermal compression.

this alloy could be represented by a schematic diagram, as demonstrated in **Figure 9**. Above the theoretical temperature of DRV, as the strain rate increases, the rate of dislocation proliferation increases and the activation energy of DRV can gradually increase. And then dynamic recovery (DRV) begins to occur until strain rate increasing to $\dot{\epsilon}_c$ (the critical strain rate at which DRV begins). According to the above experimental results, the content of α phase by aging treatment was the highest at this temperature. So it could be considered that the activation energy of α/β phase transition was the highest when $\dot{\epsilon} = 0$. And the activation energy decreases gradually with the increase of strain rate. At $\dot{\epsilon}_b$ (the strain rate at which the activation energies of DRV and phase transition are equal) the activation energies are equal, and the equilibrium state is reached. Therefore, when the greater the strain rate is, the greater the driving force is, and the recovery behavior of the β matrix mainly occurs, so that the recovery takes up the position of the second phase nucleation (Lenain et al., 2005).

Generally, when the α/β phase interface on the β grain boundary is a non-coherent interface, the α phase crystal nucleus grows in a double spherical crown shape, which can reduce the interface energy. When a part of the α/β interface maintains the Burgers orientation relationship (BOR), it maintains a flat interface while the other side grows in a spherical crown. Crystal materials are deformed at high temperatures, and there are usually two mechanisms to coordinate macroscopic deformation, namely dislocation slip and grain boundary slip. As the strain rate decreases, the effect of grain boundary sliding becomes more prominent, which causes more α phase and adjacent β matrix to fail to maintain BOR. Hua et al. (2014) found that the near- β -type Ti-5553 alloy does not strictly follow BOR between α phase and β phase after thermal deformation. From the experimental results, most of α phase and β matrix deviate from the BOR under thermal coupling, so forming equiaxed or short rod α_{GB} .

The α phase nucleation at the β grain boundary under thermal coupling tends to grow into a spherical shape rather than a lamellar shape because the α/β non-coherent interface has a high interfacial energy. In contrast, in the heat-treated sample, α phase

grows in a lamellar shape because it maintains the BOR with the α phase and has a coherent/semi-coherent phase interface (Shi et al., 2016). The α layer grows up by the accumulation of atoms on the non-coherent surface of the tip, and the migration of the coherent/semi-coherent plane increases the thickness of the α layer.

The schematic diagram of the microstructure evolution of aging heat treatment and thermal deformation of the original solution treatment sample was shown in **Figure 10**. During the aging process of Ti-5.5Mo-6V-7Cr-4Al-2Sn-1Fe alloy, as shown in **Figure 10B**, α phase nucleates in the preferential crystal, and then nucleates at the grain boundary. Since the sample produce defects and sub-grains after high-temperature forging, although the solution treatment eliminates the deformation zone, the positions of the original deformation zone or sub-grains are still retained, and the nucleation barrier is relatively low. Aging α phase is Needle-like or point-like. In the **Figure 10C**, the grains are obviously elongated under the thermal coupling, and the α phase precipitates less, mainly distributing in the grain boundary and near the partial sub-grain boundary, which is spherical and short rod-like.

CONCLUSIONS

The thermal deformation behavior of the new near- β titanium alloy Ti-5.5Mo-6V-7Cr-4Al-2Sn-1Fe in the ($\alpha + \beta$) region was studied and characterized by flow stress curve, metallographic, SEM. The following conclusions can be drawn from the present study:

- (1) Deformation temperature and strain rate can significantly affect the thermal deformation behavior. The flow stress increases with the decrease of deformation temperature and the increase of deformation rate (Reviewer 2). The flow softening process is affected by DRV, DRX and α phase spheroidization.
- (2) During the thermal deformation process, the α phase content decreases with the increase of the strain rate and the size of

α phase decreases with increasing temperature. α_{GB} is short rod or spherical. And α phase precipitated after short-term aging preferentially nucleated within the grains, which could be related to the deformation zone and the sub-grain formed during former high temperature deformation.

- (3) Compared with the aging heat treatment, thermo-mechanical processing does not induce the α phase generation, which may be due to the suppression of DS IPT by DRV.

DATA AVAILABILITY STATEMENT

The datasets generated for this study are available on request to the corresponding author.

REFERENCES

- Bai, X. F., Zhao, Y. Q., Zeng, W. D., Jia, Z. Q., and Zhang, Y. S. (2014). Characterization of hot deformation behavior of a biomedical titanium alloy TLM. *Mater. Sci. Eng. A* 598, 236–243. doi: 10.1016/j.msea.2014.01.005
- Bergström, Y. (1970). A dislocation model for the stress-strain behaviour of polycrystalline α -Fe with special emphasis on the variation of the densities of mobile and immobile dislocations. *Mater. Sci. Eng.* 5, 193–200. doi: 10.1016/0025-5416(70)90081-9
- Chai, L., Luan, B., Murty, K. L., and Liu, Q. (2013). Effect of predeformation on microstructural evolution of a Zr alloy during 550–700°C aging after β quenching. *Acta Mater.* 61, 3099–3109. doi: 10.1016/j.actamat.2013.02.001
- Chang, H., Zeng, W., Luo, Y., Zhou, Y., and Zhou, L. (2006). Phase transformation and microstructure evolution in near β Ti-B19 titanium alloy during aging treatment. *Rare Metal Mater. Eng.* 20, 1389–1392.
- Chen, L., Li, J., Zhang, Y., Lu, W., Zhang, L.-C., Wang, L., et al. (2016). Effect of low-temperature pre-deformation on precipitation behavior and microstructure of a Zr-Sn-Nb-Fe-Cu-O alloy during fabrication. *J. Nuclear Sci. Technol.* 53, 496–507. doi: 10.1080/00223131.2015.1059776
- Dehghan-Manshadi, A., and Dippenaar, R. J. (2012). Strain-induced phase transformation during thermo-mechanical processing of titanium alloys. *Mater. Sci. Eng. A* 552, 451–456. doi: 10.1016/j.msea.2012.05.069
- Estrin, Y., and Mecking, H. (1984). A unified phenomenological description of work hardening and creep based on one-parameter models. *Acta Metallurg.* 32, 57–70. doi: 10.1016/0001-6160(84)90202-5
- Fan, J., Li, J., Zhang, Y., Kou, H., Germain, L., Siredey-Schwaller, N., et al. (2017). Microstructure and crystallography of α phase nucleated dynamically during thermo-mechanical treatments in metastable β titanium alloy. *Adv. Eng. Mater.* 19:1600859. doi: 10.1002/adem.201600859
- Hua, K., Xue, X., Kou, H., Fan, J., Tang, B., and Li, J. (2014). Characterization of hot deformation microstructure of a near beta titanium alloy Ti-5553. *J. Alloys Compounds* 615, 531–537. doi: 10.1016/j.jallcom.2014.07.056
- Jonas, J. J., Aranas, C. Jr., Fall, A., and Jahazi, M. (2017). Transformation softening in three titanium alloys. *Mater. Design* 113, 305–310. doi: 10.1016/j.matdes.2016.10.039
- Jones, N. G., and Jackson, M. (2013). On mechanism of flow softening in Ti–5Al–5Mo–5V–3Cr. *Mater. Sci. Technol.* 27, 1025–1032. doi: 10.1179/026708310X12668415533720
- Lenain, A., Clément, N., Jacques, P. J., and Véron, M. (2005). Characterization of the α phase nucleation in a two-phase metastable β titanium alloy. *J. Mater. Eng. Perform.* 14, 722–727. doi: 10.1361/105994905X75510
- Liang, H. Q., Hongzhen, G., Yang, N., Chun, Q., Xiaona, P., and Zhang, J. (2014). The construction of constitutive model and identification of dynamic softening mechanism of high-temperature deformation of Ti–5Al–5Mo–5V–1Cr–1Fe alloy. *Mater. Sci. Eng. A* 615, 42–50. doi: 10.1016/j.msea.2014.07.050
- Luo, J., Liu, S. F., and Li, M. Q. (2015). Quantitative analysis of microstructure and deformation mechanisms during isothermal compression of Ti–5Al–5Mo–5V–1Cr–1Fe alloy. *Mater. Character.* 108, 115–123. doi: 10.1016/j.matchar.2015.09.003

AUTHOR CONTRIBUTIONS

JG did all the experiments and analyzing experimental statistics, as well as wrote down the research article. JC designed the research idea. JL, ZD, WZ, SY, and ZY advised the research work.

FUNDING

This work was financially supported by the National Natural Science Foundation of China (No. 51901193), Key Research and Development Program of Shaanxi (Program No. 2019GY-151), Science and Technology Plan Project of Weiyang District in Xi'an City (201902), and State Key Laboratory of Powder Metallurgy, Central South University, Changsha, China. JC was the leader of the funding.

- Matsumoto, H., Kitamura, M., Li, Y., Koizumi, Y., and Chiba, A. (2014). Hot forging characteristic of Ti–5Al–5V–5Mo–3Cr alloy with single metastable β microstructure. *Mater. Sci. Eng. A* 611, 337–344. doi: 10.1016/j.msea.2014.06.006
- Mecking, H., and Kocks, U. F. (1981). Kinetics of flow and strain-hardening. *Acta Metallurg.* 29, 1865–1875. doi: 10.1016/0001-6160(81)90112-7
- Mitchell, T. E., Hirth, J. P., and Misra, A. (2002). Apparent activation energy and stress exponent in materials with a high Peierls stress. *Acta Mater.* 50, 1087–1093. doi: 10.1016/S1359-6454(01)00409-8
- Ning, Y. Q., Luo, X., Liang, H. Q., Guo, H. Z., Zhang, J. L., and Tan, K. (2015). Competition between dynamic recovery and recrystallization during hot deformation for TC18 titanium alloy. *Mater. Sci. Eng. A* 635, 77–85. doi: 10.1016/j.msea.2015.03.071
- Qin, P., Liu, Y., Sercombe, T. B., Li, Y., Zhang, C., Cao, C., et al. (2018). Improved corrosion resistance on selective laser melting produced Ti–5Cu alloy after heat treatment. *ACS Biomater. Sci. Eng.* 4, 2633–2642. doi: 10.1021/acsbomaterials.8b00319
- Sakaki, H., Matsumiya, T., Kusumi, A., Imaizumi, T., Satoh, H., Yoshida, H., et al. (1994). Instability and flow localization during compression of a flow softening material. *J. Mater. Eng. Perform.* 3, 514–526. doi: 10.1007/BF02645318
- Shi, R., Dixit, V., Viswanathan, G. B., Fraser, H. L., and Wang, Y. (2016). Experimental assessment of variant selection rules for grain boundary α in titanium alloys. *Acta Mater.* 102, 197–211. doi: 10.1016/j.actamat.2015.09.021
- Warchomicka, F., Poletti, C., and Stockinger, M. (2011). Study of the hot deformation behaviour in Ti–5Al–5Mo–5V–3Cr–1Zr. *Mater. Sci. Eng. A* 528, 8277–8285. doi: 10.1016/j.msea.2011.07.068
- Zhang, C., Lü, Z., Wu, J., Guo, C., Zhang, S., Han, J., et al. (2019). Hot deformation behavior and microstructure evolution of a new near β titanium alloy reinforced with trace TiCp. *Adv. Eng. Mater.* 21:1800747. doi: 10.1002/adem.201800747
- Zhang, L.-C., and Chen, L.-Y. (2019). A review on biomedical titanium alloys: recent progress and prospect. *Adv. Eng. Mater.* 21:1801215. doi: 10.1002/adem.201801215
- Zurob, H. S., Hutchinson, C. R., Brechet, Y., and Purdy, G. (2014). Hot deformation characteristics of a nitride strengthened martensitic heat resistant steel. *Mater. Sci. Eng. A* 590, 199–208. doi: 10.1016/j.msea.2013.10.020

Conflict of Interest: The authors declare that the research was conducted in the absence of any commercial or financial relationships that could be construed as a potential conflict of interest.

Copyright © 2020 Gai, Cheng, Li, Du, Zhang, Yu and Yu. This is an open-access article distributed under the terms of the Creative Commons Attribution License (CC BY). The use, distribution or reproduction in other forums is permitted, provided the original author(s) and the copyright owner(s) are credited and that the original publication in this journal is cited, in accordance with accepted academic practice. No use, distribution or reproduction is permitted which does not comply with these terms.